



Photocatalytic Decolorization of BR18 and RR180 Dyes by Semiconductor Diode Laser Using CuO for Wastewater Treatment

Baris Polat · Zeynep Bilici · Yasin Ozay ·
Ibrahim Kucukkara · Nadir Dizge

Received: 4 April 2022 / Accepted: 13 July 2022 / Published online: 29 July 2022
© The Author(s), under exclusive licence to Springer Nature Switzerland AG 2022

Abstract In this study, the use of copper(II) oxide (CuO) powders as catalyst and continuous wave (CW) multimode semiconductor diode laser (450 nm) was investigated for decolorization of Basic Red 18 (BR18) and Reactive Red 180 (RR180) aqueous dye solutions. The effects of laser power (0.5–2.5 W), pH of solution (2–10), CuO catalyst loading (0.25–1.50 g/L), H₂O₂ concentration (0.28–2.22 mg/L), initial dye concentration (20–60 mg/L) were studied systematically. Maximum removal efficiency was observed as 100% for RR180 and 94.34% for BR18 under the optimum conditions. Kinetic analysis of BR18 and RR180 dye decolorization reaction indicated that the overall rate order of the reaction was the pseudo first order. CuO demonstrated satisfactory reuse capability as the catalyst for five consecutive cycles without any decrease in its activity for RR180 dye.

Keywords Semiconductor Diode Laser · BR18 · RR180 · Dye Decolorization

B. Polat · I. Kucukkara
Department of Physics, Mersin University, Mersin 33343,
Turkey

Z. Bilici · N. Dizge (✉)
Department of Environmental Engineering, Mersin
University, 33343 Mersin, Turkey
e-mail: ndizge@mersin.edu.tr

Y. Ozay
Department of Environmental Protection Technologies,
Tarsus University, Mersin, Turkey

1 Introduction

Organic and inorganic pollution originate from domestic sewage, industrial effluents, urban runoff, and agriculture wastewater. Some of the organic and inorganic pollutants can be toxic for organisms due to their environmental persistence and ability to bioaccumulation (Ali et al., 3; Langenbach, 18). Efficient treatment techniques such as precipitation, coagulation/flocculation, adsorption, ion exchange, membrane filtration, ozonation, and advanced oxidation processes for the removal of organic and inorganic pollutants from wastewater continue to attract great interest (Rashed, 25).

In recent years, photocatalytic degradation has gained great attention for the removal of organic and inorganic contaminants due to their high removal efficiency and low energy requirement (Pirilä et al., 2015). The most frequently used broad-spectrum radiation sources and photocatalyst are UV lamps and TiO₂. However, the requirement of a longer exposure time for adequate degradation and the less photonic efficiency of the UV lamps make laser-induced photocatalytic degradation preferable (Gayaa and Abdullah, 2008). Because the laser light is more consistent, monochromatic, and directive, the adsorption efficiency of the photons released from the laser beam by a photocatalyst is higher compared to photons from conventional UV lamps.

In a study, Photo degradation experiments were carried out under visible light irradiation for Rhodamine B (RhB). Results showed that visible light photocatalytic efficiency increased with laser ablation (Zhang et al., 29). In another study, photocatalytic degradation of methylene blue (MB) with Ag/AgCl catalyst was investigated with diode lasers (443 nm blue-light) as alternative light sources. Moreover, 440–450-nm LED light source (1 W) was used as control. The effects of different parameters such as laser energy (0–1.15 W), light source, initial dye concentration (4–20 mg/L), catalyst loading (0.2–1.8 g/L), and pH (3–12) were investigated on decolorization and degradation. It was reported that the decolorization and degradation of MB increased when the laser energy increased and 100% decolorization and 90% degradation of MB achieved in 10 min under optimum conditions (pH 9.63, 4 mg/L MB concentration, 1.4 g/L catalyst amount) (Liu et al., 19). Degradation of organic pollutants was also studied under visible laser light in a study. Neodymium-doped Yttrium Aluminum Garnet (Nd-YAG) 532 nm laser light (10 to 2230 mW) and green LED light (100 mW) were compared for degradation of Bisphenol A in time of 0–15 irradiation by using Au/TiO₂, Au/Al₂O₃, Au/ZnO, and TiO₂ as photocatalyst. It was reported that when laser light and LED light were used at the same power (100 mW), laser light showed more efficiency on electron transfer (Chehadi et al., 8). However, for some studies, laser light may not be optimal light source for photo degradation process. Amoli-Diva et al., (4) synthesized TiO₂-modified Fe₃O₄ nanocomposite by laser reduction method for photo degradation of rhodamine-6G (Rh6G), and they compared laser light (405 nm) and xenon lamp for photocatalytic activity. Also, the effect of various parameters such as pH, photocatalyst concentration, type of catalyst was studied on the degradation efficiency of Rh6G. Results showed that the photocatalysts had higher photocatalytic performance with xenon light source in comparison with laser light (405 nm). In another study, Nd-YAG laser (532 nm) was used for synthesis of graphene TiO₂ nano hybrid catalyst. Irradiation conditions were 320 mJ/pulse with laser pulse duration of 6 ns and repetition rate of 10 Hz for 45 min. They reported that removal efficiency of methyl orange (MO) increased from 89.10 to 99.60% when 500-W Xenon lamp was used (Ilyas

et al., 16). Baig et al. (5) used Nd-YAG laser (Brilliant B) for synthesis of g-C₃N₄-CdS nanocomposites, and photocatalytic degradation of MB and RhB from aqueous solutions was carried out. It was reported that high photocatalytic activity was achieved under visible light irradiation.

Different shapes of nanostructured hematite (α -Fe₂O₃) synthesized by pulsed laser deposition were compared for photocatalytic water purification. In ablation process, KrF excimer laser (248 nm) was used at 3 J/cm², pulse duration of 25 ns, and repetition rate of 20 Hz. In another study, WO₃ nanoparticles synthesized by pulsed laser (Nd-YAG) ablation were investigated for antibacterial properties and photocatalytic activity. Different laser fluencies (13 to 23 J/cm²) were used for ablation process (Fakhari et al., 2018). Laser-modified TiO₂/SnO₂ powders decorated with SiC nanocrystals were tested for photocatalytic activity (Zhang et al., 29). For determining photocatalytic activity of products, experiments were carried out with Rh B by using 80-W halogen lamp (340–850 nm) and 125-W mercury lamp (253 nm) for 2 h. Antibacterial activity of products was tested against *Escherichia coli* bacteria. The products synthesized with 23 J/cm² supplied the highest efficiency. In another study, tungsten oxide/reduced graphene oxide (WO₃-rGO) nanocomposite catalyst has been synthesized by pulsed laser ablation method. Experimental studies showed that WO₃-rGO had better photocatalytic activity when compared to pure WO₃ for degradation of MB dye in water (Ibrahim et al., 15).

In this study, the use of copper(II) oxide (CuO) powders as catalyst and continuous wave (CW) multi-mode semiconductor diode laser (450 nm) was investigated for decolorization of Basic Red 18 (BR18) and Reactive Red 180 (RR180) aqueous dye solutions. The effects of laser power, solution pH, catalyst amount, and H₂O₂ concentration were tested on dye decolorization. Moreover, kinetic study and reusability of the catalyst were also studied.

2 Materials and Methods

2.1 Chemicals and Analyses

CuO was supplied from Tekkim (CAS: 1317–38–0). Basic Red 18 (BR18) and Reactive Red 180

(RR180) dyes were obtained from Dystar. BR18 is a cationic azo dye used for coloring textiles. The chromophore is the cation, which contains many functional groups, but most prominently the quaternary ammonium center (Hunger et al., 14). RR180 is an anionic single azo class dye (Lingeswari & Vimala, 20). Some important properties of the dyes are shown in Table 1.

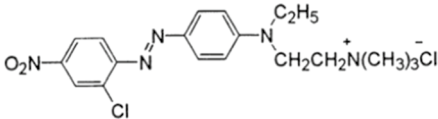
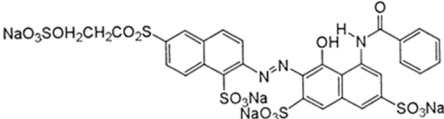
CuO catalyst was characterized by SEM–EDX. Scanning electron microscopy (SEM) was used to observe the surface morphology of the catalyst (SEM, Zeiss Supra 55, Germany). The energy-dispersive X-ray spectroscopy (EDX) was utilized to quantify the composition of the elements present on the catalyst's surface. The CuO powder was characterized by X-ray diffraction (XRD), using $\text{CuK}\alpha$ radiation with $\lambda=0.15406$ nm, employing a Shimadzu XRD 6000 diffractometer operated at 30 mA and 40 kV, in the 2θ range from 10 to 90° , with a scan speed of $4^\circ/\text{min}$. The specific surface areas of CuO powders were measured using nitrogen adsorption at 77 K (ASAP-2020, Micromeritics), with calculation according to the Brunauer–Emmett–Teller (BET) method. The zeta potentials of dilute suspensions of CuO powders were measured with a Zeta Sizer nano-ZS instrument (Malvern Instruments), in the pH range from 2 to 10, with the pH adjusted by adding 0.1 M HCl or 0.1 M NaOH.

2.2 Experimental Configuration for Photocatalytic Decolorization

In this study, a continuous wave (CW) 450-nm multi-mode semiconductor diode laser (Thorlabs/L450G1) was used. A power meter (Thorlabs/PM100) was used to measure the optimum laser output power value. The laser was controlled by a laser combi controller (Thorlabs/ITC-4005). The detailed experimental procedure can be found elsewhere (Polat et al., 24). The specifications of the laser diode, the laser combi controller, and the TEC used in the laser-assisted disinfection system are described in detail elsewhere (Polat et al., 24).

3D drawing of the experimental setup is shown in Fig. 1. The experiments were carried out in a glass beaker (GB). A magnetic bar (MB) and magnetic stirrer (MS) were used for mixing the dyes in the GB. The aluminum platform (AP) was used for both the assembly platform and heat sink. Laser tube (LT) was used for collimating and saving of laser diode chip. The laser diode chip (LC) was used as a light source for photocatalytic decolorization. The laser head (LH) was used to keep the stable temperature of the LC. Two houses namely the house of laser tube (HLT) and the house of heat sensor (HHS) were opened to the surface of the LH for putting of the LT and a heat sensor (HS, Thorlabs—AD590). Copper plate (CP) was used for transferring heat load on the TEC. The TEC was used to

Table 1 Some important properties of the dyes

Dye name	Chemical structure	Formula and	UV
		Molecular weight (g/mol)	absorption λ_{max} (nm)
Basic Red 18 (BR18)		$\text{C}_{19}\text{H}_{25}\text{Cl}_2\text{N}_5\text{O}_2$ 426.34 g/mol	484
Reactive Red 180 (RR180)		$\text{C}_{29}\text{H}_{19}\text{N}_3\text{Na}_4\text{O}_{17}\text{S}_5$ 937.79 g/mol	542

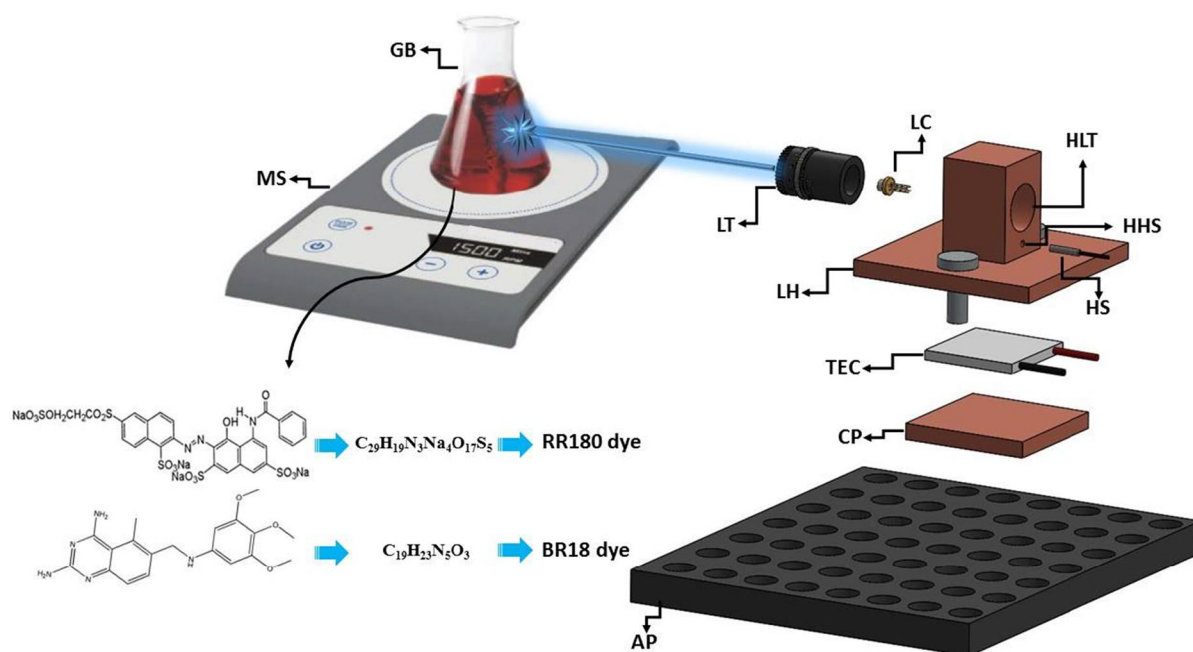


Fig. 1 3D explosion view of the experimental setup configuration for photocatalytic decolorization

keep the stable temperature of the LC, and finally, the HS was used to measure the LCC temperature instantaneously.

2.3 Photocatalytic Decolorization with Diode Laser

First, LT was placed into the HLT. The TEC was placed under the HLT, and it was controlled by the LCC with 1 A. Measuring the LC temperature was made by the HS connected to the LCC. Then, the LC and the temperature were controlled by the LCC. After the controlling of their temperature, photocatalytic decolorization studies were started for both BR18 and RR180 dyes, respectively.

In the experiments, the condition in which the elimination reaches the optimum value according to the varying values depending on the various parameters was examined. These parameters are as follows: laser power, solution pH, CuO catalyst amount, H_2O_2 concentration, dye (BR18 and RR180) concentration, and kinetic studies. The reusability stability of CuO catalyst was tested individually for each dye. The optimization was achieved step by step changing only one parameter while keeping other parameters constant for 3 h in each experiment.

3 Results and Discussion

3.1 SEM Images of the Catalyst

SEM images of the CuO catalyst are shown in Fig. 2. SEM–EDX technique was used to investigate the morphology of the catalyst. The catalyst had an irregular cubic shape with smooth surface. The EDX analysis of the catalyst showed that the elementary components were only composed of Cu and O.

CuO powder was also characterized by XRD analysis (Fig. 3). Consistent with the peaks of the CuO standard PDF-2 01–080–1268, 32.56° CuO 110 peak, 35.48° CuO 002 peak, 35.59° CuO–111 peak, 38.77° CuO 111 peak, 46.28° CuO–211 peak, 48.78° CuO–202 peak, 53.50° CuO 020 peak, 58.37° CuO 202 peak, 61.58° CuO–113 peak, 68.16° CuO 113 peak, 72.48° CuO 311 peak, 75.31° CuO–222 peak, 80.23° CuO–204 peak were detected (Bouazizi et al., 6; Zhu et al., 30). The peaks of CuO were determined to be pure CuO, and the sharp diffraction peaks indicate that the CuO was monoclinic.

Zeta potential analysis was performed to determine the CuO surface charge characteristics as a function of pH. Figure 4 shows CuO zeta potential plotted as a function of pH, with a predominantly positive charge

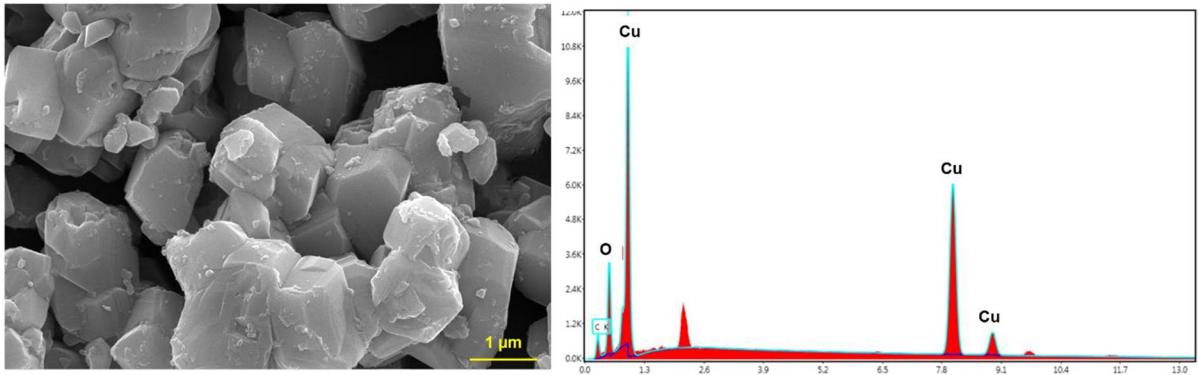


Fig. 2 SEM and EDX spectra of the CuO catalyst

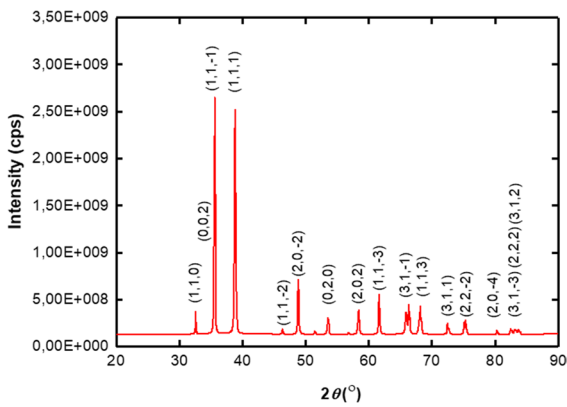


Fig. 3 XRD pattern of the CuO catalyst

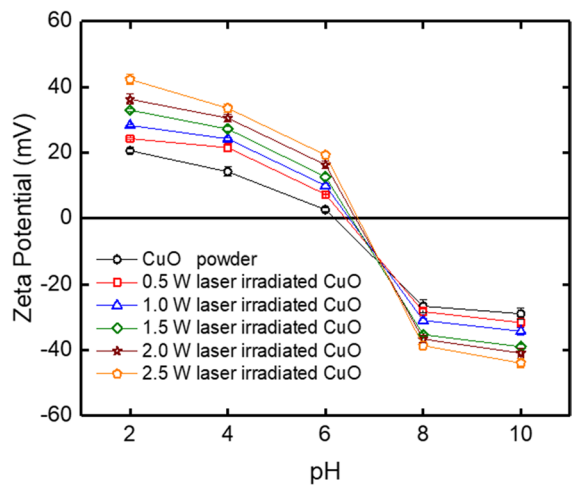


Fig. 4 Zeta potential values of CuO powder and laser irradiated CuO with different laser power

density in an aqueous medium. The isoelectric point (IEP) of the CuO was at pH:6.1. However, laser irradiation changed IEP of the CuO, and IEP increased from 6.4 to 6.8 mV when laser irradiation was increased from 0.5 to 2.5 W. Moreover, zeta potential increased after laser irradiation compared to raw CuO powder.

The Brunauer–Emmett–Teller (BET) equation was used to determine the surface area, pore volume, and pore size distributions using the Barret–Joyner–Halenda (BJH) model. The BET results

Table 2 Summary BET data of the CuO powder before and after laser irradiation

Sample	BET surface area (m ² /g)	Pore volume (cm ³ /g)	Pore size (nm)
CuO powder	0.4759	0.00039	63.7896
0.5 W laser irradiated	0.6117	0.00100	12.0739
1.0 W laser irradiated	0.7663	0.00125	9.3021
1.5 W laser irradiated	1.1344	0.00171	8.1103
2.0 W laser irradiated	1.4490	0.00230	7.6574
2.5 W laser irradiated	1.9328	0.00256	5.7898

are shown in Table 2. It was observed that laser irradiation had a great impact on surface area and pore-size distribution. The surface area was low for the raw CuO powder ($0.4759 \text{ m}^2/\text{g}$). In contrast, laser irradiated CuO could dramatically increase their surface area with a maximum of $1.9328 \text{ m}^2/\text{g}$ as the irradiated power of laser increased to 2.5 W. The laser irradiation process caused a pore size distribution between 1 and 100 nm with obviously increased pore volume.

3.2 The Effect of Laser Power on Dye Decolorization

The photocatalytic decolorization of BR18 and RR180 dyes with diode laser was performed in the range of 0.5–2.5 W using CuO catalyst, and the results are given in Fig. 5. The results depicted that RR180 dye was decolorized more efficiently than BR18 dye. The dye removal efficiencies increased from 36.14 to 94.34% for BR18 dye and from 74.34 to 100% for RR180 dye when laser power increased from 0.5 to 2.5 W. However, RR180 dye enhanced complete dye removal at laser power of 1.5 W for 60 min.

3.3 The Effect of Solution pH on Dye Decolorization

The effect of solution pH in the range of 2–10 was investigated on dye decolorization using diode laser, and the results are shown in Fig. 6. The maximum removal efficiencies were obtained 94.34% and 100%

for BR18 and RR180 dyes, respectively, at pH 6.0 for 60 min. Lower removal efficiencies were obtained out the range of pH 6.0. The solution pH may have mainly caused modification of the electrical double layer of the solid-electrolyte interface, and accordingly varying electrostatic interactions may have affected decolorization of the dyes (Liu et al., 2013). As the pH of the solution increased from 6 to 10, the number of positively charged CuO catalyst sites decreased, and the number of negatively charged surface sites increased. These conditions (beyond pH 6) non favor the adsorption of positively charged BR18 cations and negatively charged RR180 anions. Moreover, the reduced decolorization of BR18 at acidic pH might be due to the presence of excess H^+ ions, which compete with BR18 cations for available adsorption sites.

3.4 The Effect of Catalyst Amount on Dye Decolorization

The effect of CuO amount for photocatalytic decolorization of BR18 and RR180 dyes with diode laser performed in the range of 0.1–1.5 g/L is given in Fig. 7. The results showed that decolorization of RR180 dye was more efficient than BR18 dye. The maximum dye removal efficiencies were obtained 94.34% at 0.5 g/L for BR18 dye and 100% at 0.25 g/L for RR180 dye. The rate of dye decolorization remained almost constant beyond 0.5 g/L catalyst loading. The interaction

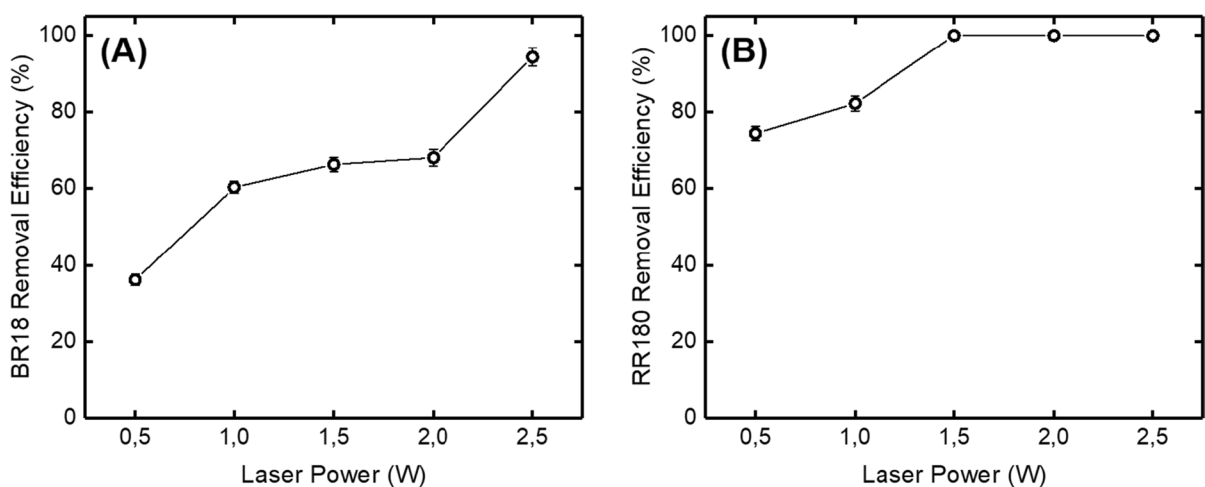


Fig. 5 The effect of laser power on dye decolorization (experimental conditions: catalyst amount: 0.5 g/L; H_2O_2 concentration: 1.11 mg/L; dye concentration: 20 mg/L; pH: 6.0; volume: 50 mL)

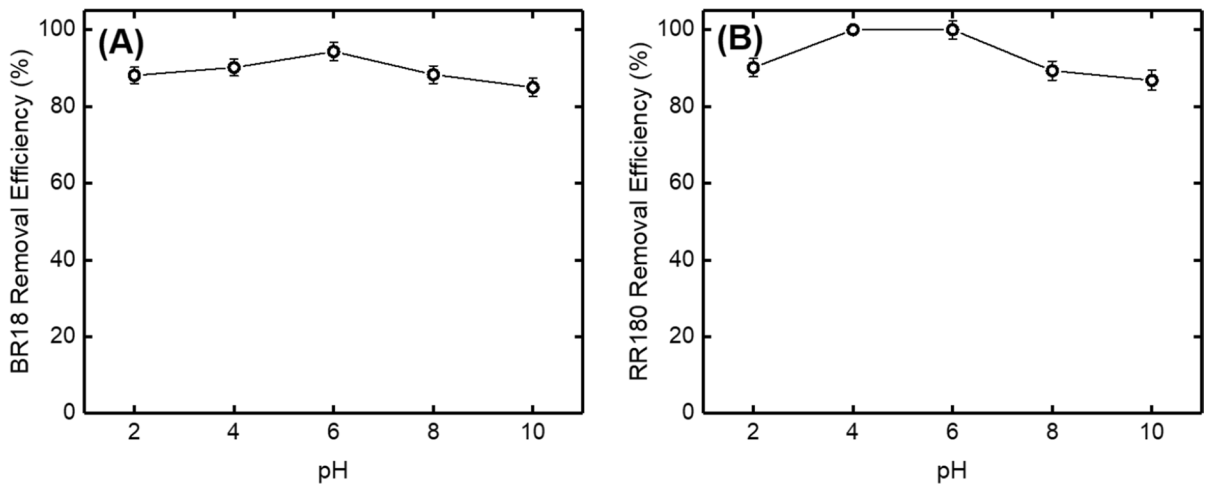


Fig. 6 The effect of solution pH on dye decolorization (experimental conditions: CuO catalyst amount: 0.5 g/L; H₂O₂ concentration: 1.11 mg/L; dye concentration: 20 mg/L; laser power: 2.5 W; volume: 50 mL)

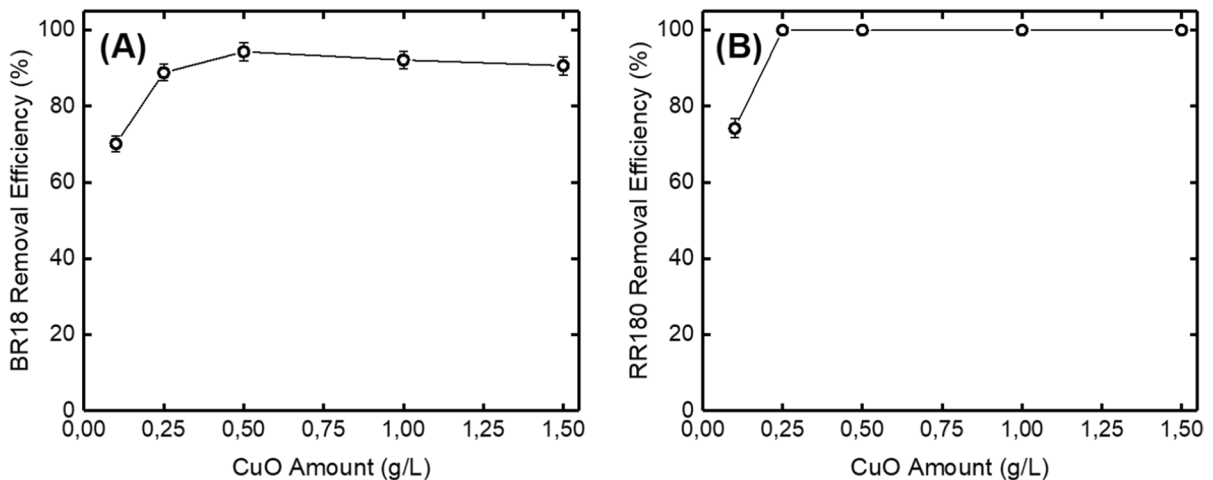


Fig. 7 The effect of catalyst amount on dye decolorization (experimental conditions: H₂O₂ concentration: 1.11 mg/L; dye concentration: 20 mg/L; solution pH 6.0; laser power: 2.5 W; volume: 50 mL)

between the initial dye concentration and the available catalyst sites can affect the dye decolorization rate. When total active surface area increases on the catalyst surface, availability of more active sites increases (Akyol et al., 2). In addition, more catalyst can cause increase in turbidity of the suspension with high dose of photocatalyst, which can cause a decrease in penetration of laser light and hence decolorization efficiency can decrease (Daneshvar et al., 9). Therefore, the catalyst dose of 0.5 g/L was fixed for further studies.

3.5 The Effect of H₂O₂ Concentration on Dye Decolorization

Since there was 94.34% BR18 dye removal with CuO catalyst at 20 mg/L dye concentration, H₂O₂ was added to the solution and laser was applied. The effect of H₂O₂ concentration on BR18 and RR180 dye removal is given in Fig. 8. As it is well known, H₂O₂ forms OH• radicals by photolysis reaction with UV irradiation, and these OH• radicals increase photocatalytic oxidation.

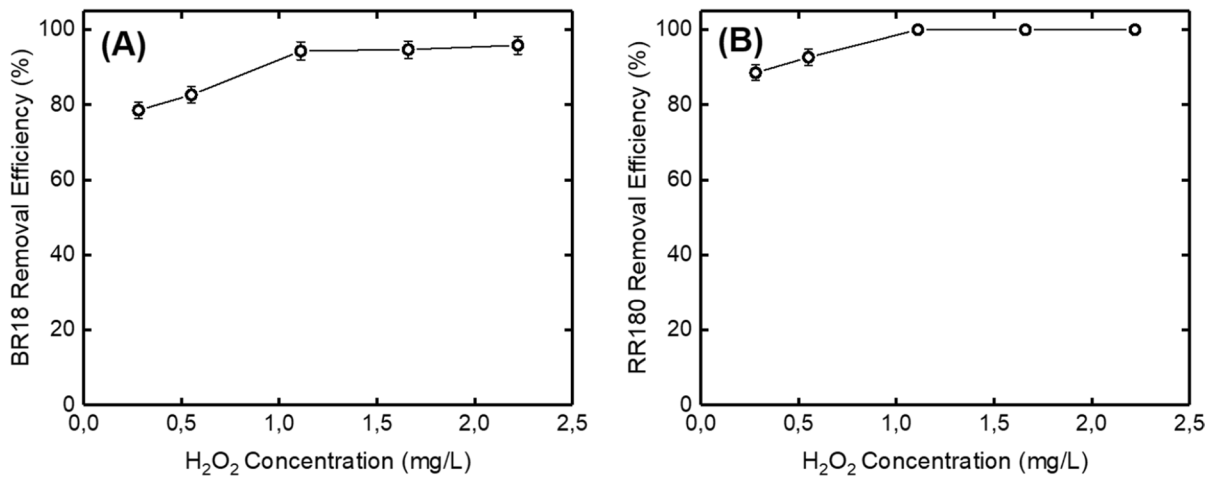


Fig. 8 The effect of H₂O₂ concentration on dye decolorization (experimental conditions: CuO catalyst amount: 0.5 g/L; dye concentration: 20 mg/L; solution pH: 6.0; laser power: 2.5 W; volume: 50 mL)

BR18 removal efficiency increased quite a few when H₂O₂ concentration increased. However, 1.11 mg/L H₂O₂ concentration was enough to decolorize all RR180 dye, and it did not observe more dye removal when more H₂O₂ was added into the reaction medium. This is due to excessive H₂O₂ addition preventing OH[•] formation and sweeping effect. The addition of H₂O₂ as electron acceptor significantly enhanced the decolorization process. Moreover, two decolorization mechanisms may be simultaneously occurring in the system, namely, direct decomposition and catalytic decomposition (Liu et al., 2013). In the first decolorization mechanism, the photons are directly absorbed by dye molecules; the absorption results in the initiation of the bond breakage. In the second decolorization mechanism, the photons are first absorbed by the CuO catalyst, and the generated free OH[•] radicals break the bonds of the dyes.

In the laser decolorization process, the effects of laser, H₂O₂ concentration, and CuO catalyst amount on individual BR18 and RR180 dye removal were also investigated. It was seen that laser and catalyst alone were not effective in BR18 and RR180 dye removal, and all removal was due to laser decolorization with H₂O₂ and CuO catalyst (Fig. 9). H₂O₂ degraded the BR18 and RR180 dyes 19.3% and 52.9% under diode laser, respectively. In addition, 100% and 94.34% removal efficiencies were obtained for RR180 and BR18 dyes, respectively, when H₂O₂

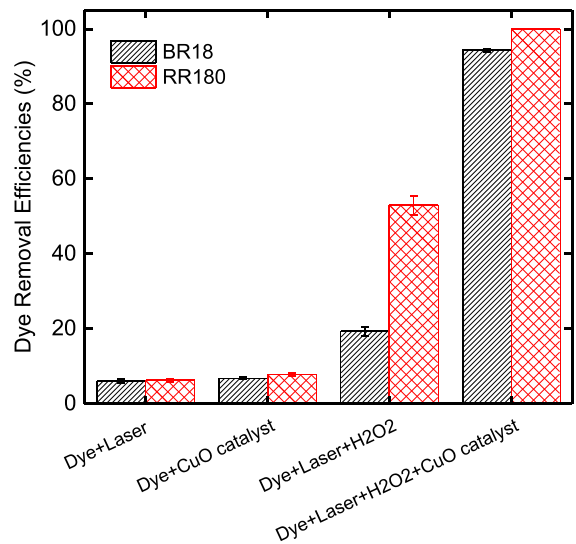


Fig. 9 The effect of laser, H₂O₂ concentration, and CuO catalyst on laser decolorization process (experimental conditions: dye concentration: 20 mg/L; CuO catalyst amount: 0.5 g/L; H₂O₂ concentration: 1.11 mg/L; solution pH: 6.0; laser power: 2.5 W; volume: 50 mL)

and CuO catalysts were added into the reaction medium under laser irradiation.

3.6 Kinetic Study

The effect of initial dye concentration on the decolorization efficiency is given in Fig. 10 for different

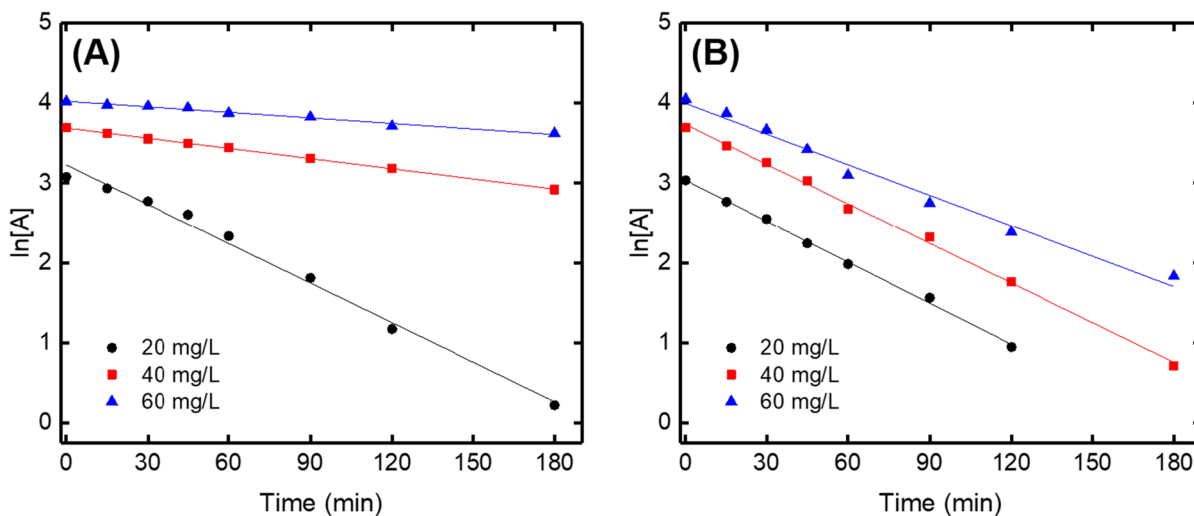


Fig. 10 Kinetic study of BR18 and RR180 dye decolorization with diode laser (experimental conditions: CuO catalyst amount: 0.5 g/L; H₂O₂ concentration: 1.11 mg/L; solution pH: 6.0; laser power: 2.5 W; volume: 50 mL)

Table 3 The correlation coefficients and the rate constant for decolorization of BR18 and RR180 dyes

Dye	Zero order		First order		Second order	
	k_0 (mg/L min)	R^2	k_1 (1/min)	R^2	k_2 (L/mg min)	R^2
BR18						
20 mg/L	0.1188	0.9174	0.0165	0.9912	0.0039	0.8434
40 mg/L	0.1184	0.9888	0.0042	0.9994	0.0002	0.9831
60 mg/L	0.1059	0.9798	0.0023	0.9847	0.00005	0.9843
RR180						
20 mg/L	0.1090	0.8662	0.0171	0.9975	0.0027	0.9025
40 mg/L	0.2054	0.8668	0.0165	0.9975	0.0024	0.8321
60 mg/L	0.2818	0.8511	0.0127	0.9853	0.0008	0.9602

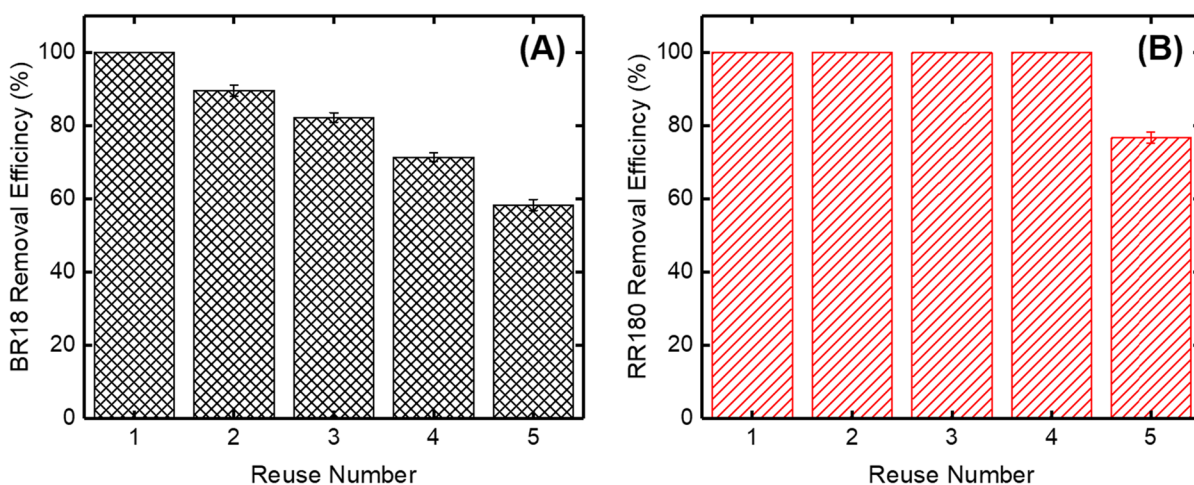


Fig. 11 Reuse stability of BR18 and RR180 dye decolorization with diode laser (experimental conditions: CuO catalyst amount: 0.5 g/L; H₂O₂ concentration: 1.11 mg/L; solution pH: 6.0; laser power: 2.5 W; volume: 50 mL)

Table 4 Performance comparison of CuO photocatalyst with other photocatalysts reported in the literature

Material	Dye	Conditions	Light source	Removal efficiency	Reference
CuO powder	Basic Red 18 (BR18) and Reactive Red 180 (RR180)	pH: 6.0; catalyst amount: 0.5 g/L; H ₂ O ₂ concentration: 1.11 mg/L; laser power: 2.5 W; dye concentration: 20 mg/L	450-nm multimode semiconductor diode laser	100% for RR180 and 94.34% for BR18 for 180 min	This study
Aqueous suspensions of titanium dioxide (TiO ₂)	RR180	pH: 6.4; catalyst amount: 1.142 g/L; H ₂ O ₂ concentration: 1 mM; lamp power: 250 W; dye concentration: 5 × 10 ⁻⁵ M	360–2000 nm tungsten-halogen lamp visible light	80% for 5 h	Kurtechen et al., 17
CoPc(COOH) ₄ -TiO ₂ nanocomposites	RR180	Catalyst amount: 1 g/L; dye concentration: 10 mg/L	Visible light	30% for 180 min	Dindas et al., 10
TiO ₂ powders	RR180	-	Visible light	98% for 45 min	Tuncer and Ozdemir
ZnO plates	RR180	Plate dimension: 95 mm × 40 mm; dye concentration: 20 mg/L	365-nm UV-A lamps	95.7% for 90 min	Yassitepe et al., 28
CdSe QD-ZnO nanocomposite	BR18	pH: 7.0; catalyst amount: 0.04 g/L; lamp power: 9 W; dye concentration: 20 mg/L	UV-C lamp	100% for 120 min	Mahmoodi et al., 2018
ZnO impregnated <i>Aspergillus carbonarius</i> (AC) fungi	RR180 BR18	pH: 6.9 for RR180 and 8.3 for BR18; catalyst amount: 2 g/L; dye concentration: 10 mg/L	365-nm UV-A lamps	76.2% for RR180 and 100% for BR18 for 180 min	Bouras et al., 7

concentrations of BR18 and RR180 dye solutions. The results shown in Fig. 10 indicated that the initial concentration of BR18 and RR180 could influence the decolorization process. Increasing of dye concentration from 20 to 60 mg/L engendered competing for more dye molecules on the same active sites on the catalyst surface; subsequently, the generation of OH^\bullet radicals on the surface of the catalyst was declined. Moreover, at high dye concentration, the increased color of the aqueous solution reduces the laser penetration and thereby renders the catalytic process less efficient.

The correlation coefficients and the rate constant for decolorization of BR18 and RR180 dyes are shown in Table 3. Kinetic analysis of the BR18 and RR180 dye decolorization reaction indicated that the overall rate order of the reaction was pseudo first order. Similar result was found by Liu et al. (2013). They reported that MB was decolorized rapidly at 1 min and decolorized almost completely within 15 min; the decolorization rate was about 94%.

3.7 Reuse Stability

Reuse stability of CuO catalyst was tested for BR18 and RR180 dye decolorization (Fig. 11). The results showed that no decrease in the RR180 dye removal efficiency was observed up to 4 cycles for CuO catalyst. However, BR18 dye lost its activity dramatically after 2 cycles. It can be explained that the surface area increased as the particle size of CuO decreased after laser irradiation. Thus, the electrostatic repulsion increased between the cationic BR18 dye and CuO catalyst; however, the electrostatic attraction increased between the anionic RR180 dye and CuO catalyst. This caused to decrease decolorization efficiency of BR18 dye with consecutive reuse cycle. The smaller the size, the bigger the Coulombic effect. In addition, catalyst losses over time during the separation of the catalyst from the liquid resulted in decreased decolorization of the RR180 dye after the fifth reuse. Hayat et al. (13) reported that a decrease of approximately 20% was observed in the photocatalytic activity of the nanocrystalline WO_3 catalyst after completion of the third cycle. Amoli-Diva et al. (4) reported that the efficiency of magnetically recoverable photocatalyst for the photocatalytic degradation of Rh6G still maintains 92–95%, even after 5 cycles.

Photocatalytic performance of CuO catalyst was compared with various photocatalysts reported in the literature. Our results demonstrated that the photocatalytic performance of CuO showed stable reusability and comparable efficiency for decolorization of BR18 and RR180 dyes (Table 4). Therefore, CuO catalyst can be considered as active, low-cost, easily separable, and stable photocatalyst.

4 Conclusion

In this study, continuous wave (CW) 450-nm multimode semiconductor diode laser and CuO catalyst were used for decolorization of cationic and anionic dye solutions. The results indicated that decolorization increased for both BR18 and RR180 dyes when the laser power increased. 100% RR180 dye and 94.34% BR18 dye decolorizations were achieved for 180 min under optimum conditions with solution pH of 6.0, catalyst amount of 0.5 g/L, H_2O_2 concentration of 1.11 mg/L, and laser power of 2.5 W. Performance of the catalyst was successfully maintained four successive runs for RR180 dye solutions without any decrease. It was clearly understood that diode laser can be an affective light source for decolorization of basic dye solutions.

Semiconductor diode laser can be considered as an attractive technology in the treatment of colored wastewater due to its excellent properties such as high speed, high flexibility, high sensitivity, high reliability, and less chemical use and less process steps compared to the conventional treatment process. The performance of the proposed process should be tested on long-term pilot scale systems.

Author Contribution BP and ZB performed methodology and data curation. YO performed methodology. IK performed investigation and writing—original draft. ND performed conceptualization, writing—original draft, formal analysis, and review and editing. All authors read and approved the final manuscript.

Data Availability The datasets used and/or analysed during the current study are available from the corresponding author on reasonable request.

Declarations

Ethics Approval and Consent to Participate Not applicable.

Consent for Publication Not applicable.

Competing Interests The authors declare no competing interests.

References

- Ahmed, S. M., & Imam, H. (2020). Characterization and photocatalytic activity of Eu:ZnO & Au/Eu:ZnO nanoparticles prepared by laser ablation in water. *Materials Science in Semiconductor Processing*, 115, 105128. <https://doi.org/10.1016/j.mssp.2020.105128>
- Akyol, A., Yatmaz, H. C., & Bayramoglu, M. (2004). Photocatalytic decolorization of Remazol Red RR in aqueous ZnO suspensions. *Applied Catalysis B: Environmental*, 54, 19–24.
- Ali, H., Khan, E., Iah, I. (2019). Environmental chemistry and ecotoxicology of hazardous heavy metals: Environmental persistence, toxicity, and bioaccumulation. *Hindawi Journal of Chemistry* 0–14
- Amoli-Diva, M., Anvari, A., & Sadighi-Bonabi, R. (2019). Synthesis of magneto-plasmonic Au-Ag NPs-decorated TiO₂-modified Fe₃O₄ nanocomposite with enhanced laser/solar-driven photocatalytic activity for degradation of dye pollutant in textile wastewater. *Ceramics International*, 45(14), 17837–17846. <https://doi.org/10.1016/J.CERAMINT.2019.05.355>
- Baig, U., Hawsawi, A., Ansari, M. A., Gondal, M. A., Dastageer, M. A., & Falath, W. S. (2020). Synthesis, characterization and evaluation of visible light active cadmium sulfide-graphitic carbon nitride nanocomposite: A prospective solar light harvesting photo catalyst for the deactivation of waterborne pathogen. *Journal of Photochemistry and Photobiology B: Biology*, 204, 111783. <https://doi.org/10.1016/j.jphotobiol.2020.111783>
- Bouazizi, N., Bargougui, R., Oueslati, A., & Benslama, R. (2015). Effect of synthesis time on structural, optical and electrical properties of CuO nanoparticles synthesized by reflux condensation method. *Advanced Materials Letters*, 6(2), 158–164.
- Bouras, H. D., Isik, Z., Bezirhan, E. A., Bouras, N., Chergui, A., Yatmaz, H. C., & Dizge, N. (2019). Photocatalytic oxidation of azo dye solutions by impregnation of ZnO on fungi. *Biochemical Engineering Journal*, 146, 150–159.
- Chehadi, Z., Alkees, N., Bruyant, A., Toufaily, J., Girardon, J. S., Capron, M., Dumeignil, F., Hamieh, T., Bachelot, R., & Jradi, S. (2016). Plasmonic enhanced photocatalytic activity of semiconductors for the degradation of organic pollutants under visible light. *Materials Science in Semiconductor Processing*. <https://doi.org/10.1016/j.mssp.2015.08.044>
- Daneshvar, N., Salari, D., & Khataee, A. R. (2003). Photocatalytic degradation of azo dye acid red 14 in water on ZnO as an alternative catalyst to TiO₂. *Journal of Photochemistry and Photobiology, A: Chemistry*, 157, 111–116.
- Dindaş, G. B., Şahin, Z., Yatmaz, H. C., & İşçi, Ü. (2019). Cobalt phthalocyanine-TiO₂ nanocomposites for photocatalytic remediation of textile dyes under visible light irradiation. *Journal of Porphyrins and Phthalocyanines*, 23, 561–568. <https://doi.org/10.1142/S1088424619500482>
- Fakhari, M., Torkamany, M. J., Mirnia, S. N., & Elahi, S. M. (2018). UV-visible light-induced antibacterial and photocatalytic activity of half harmonic generator WO₃ nanoparticles synthesized by Pulsed Laser Ablation in water. *Optical Materials*, 85, 491–499. <https://doi.org/10.1016/J.OPTMAT.2018.09.023>
- Hassan, M., Gondal, M. A., Cevik, E., Dastageer, M. A., Baig, U., Moqbel, R. A., Qahtan, T. F., Bozkurt, A., & Al Abass, N. (2021). Laser assisted anchoring of cadmium sulfide nanospheres into tungsten oxide nanosheets for enhanced photocatalytic and electrochemical energy storage applications. *Colloids Surfaces A Physicochem. Eng. Asp.*, 617, 126318. <https://doi.org/10.1016/j.colsurfa.2021.126318>
- Hayat, K., Gondal, M. A., Khaled, M. M., Yamani, Z. H., & Ahmed, S. (2011). Laser induced photocatalytic degradation of hazardous dye (Safranin-O) using self synthesized nanocrystalline WO₃. *Journal of Hazardous Materials*, 186(2–3), 1226–1233. <https://doi.org/10.1016/J.JHAZMAT.2010.11.133>
- Hunger, K., Mischke, P., Rieper, W., Raue, R., Kunde, K., Engelet, A. (2005) Azo Dyes. Ullmann's encyclopedia of industrial chemistry. Weinheim: Wiley-VCH. https://doi.org/10.1002/14356007.a03_245
- Ibrahim, Y. O., Gondal, M. A., Alaswad, A., Moqbel, R. A., Hassan, M., Cevik, E., Qahtan, T. F., Dastageer, M. A., & Bozkurt, A. (2020). Laser-induced anchoring of WO₃ nanoparticles on reduced graphene oxide sheets for photocatalytic water decontamination and energy storage. *Ceramics International*, 46(1), 444–451. <https://doi.org/10.1016/J.CERAMINT.2019.08.281>
- Ilyas, A. M., Gondal, M. A., Baig, U., Akhtar, S., & Yamani, Z. H. (2016). Photovoltaic performance and photocatalytic activity of facile synthesized graphene decorated TiO₂ monohybrid using nanosecond pulsed ablation in liquid technique. *Solar Energy*, 137, 246–255. <https://doi.org/10.1016/j.solener.2016.08.019>
- Kurichen, S. K., Murugesan, S., Raj, S. P., & Maruthamuthu, P. (2011). Visible light assisted photocatalytic mineralization of Reactive Red 180 using colloidal TiO₂ and oxone. *Chemical Engineering Journal*, 174(2–3), 530–538.
- Langenbach, T. (2013) Persistence and bioaccumulation of persistent organic pollutants (POPs), Applied bioremediation—Active and passive approaches, Yogesh B. Patil and Prakash Rao, IntechOpen
- Liu, Z. Y., Wang, G. Y., Liu, X. P., & Wang, Y. J. (2013). Preparation of CuCrO₂ and the photocatalytic properties of its composites. *Journal of Fuel Chemistry and Technology*, 41(12), 1473–1480. [https://doi.org/10.1016/S1872-5813\(14\)60007-4](https://doi.org/10.1016/S1872-5813(14)60007-4)
- Liu, X., Yang, Y., Shi, X., & Li, K. (2015). Fast photocatalytic degradation of methylene blue dye using a low-power diode laser. *Journal of Hazardous Materials*, 283, 267–275. <https://doi.org/10.1016/J.JHAZMAT.2014.09.031>
- Lingeswari, U. D., & Vimala, T. (2020). Adsorption study on removal of Reactive Blue 21 and Reactive Red 180 from aqueous medium using polyaniline CuCl₂ in the presence

- of UV light. *Rasayan Journal of Chemistry*, 13(3), 1544–1554. <https://doi.org/10.31788/RJC.2020.1335722>
- Mahmoodi, N. M., Karimi, B., Mazarji, M., & Moghtaderi, H. (2018). Cadmium selenide quantum dot-zinc oxide composite: Synthesis, characterization, dye removal ability with UV irradiation, and antibacterial, activity as a safe and high-performance photocatalyst. *Journal of Photochemistry and Photobiology b: Biology*, 188, 19–27.
- Naik, S. S., Lee, S. J., Begildayeva, T., Yu, Y., Lee, H., & Choi, M. Y. (2020). Pulsed laser synthesis of reduced graphene oxide supported ZnO/Au nanostructures in liquid with enhanced solar light photocatalytic activity. *Environmental Pollution*, 266, 115247. <https://doi.org/10.1016/j.envpol.2020.115247>
- Naik, S. S., Lee, S. J., Yeon, S., Yu, Y., & Choi, M. Y. (2021). Pulsed laser-assisted synthesis of metal and nonmetal-codoped ZnO for efficient photocatalytic degradation of Rhodamine B under solar light irradiation. *Chemosphere*, 274, 129782. <https://doi.org/10.1016/j.chemosphere.2021.129782>
- Pirilä, M., Saouabe, M., Ojala, S., Rathnayake, B., Drault, F., Valtanen, A., Huuhtanen, M., Brahmi, R., Keiski, R.L. (2015). Photocatalytic Degradation of Organic Pollutants in Wastewater. *Top Catal*, 58, 1085–1099. <https://doi.org/10.1007/s11244-015-0477-7>
- Polat, B., Ozay, Y., Bilici, Z., Kucukkara, İ., & Dizge, N. (2020). Membrane modification with semiconductor diode laser to reduce membrane biofouling for external MBR system and modelling study. *Separation and Purification Technology*, 241, 116747. <https://doi.org/10.1016/J.SEPPUR.2020.116747>
- Rashed, M.N. (2013). Adsorption technique for the removal of organic pollutants from water and wastewater, organic pollutants—Monitoring, risk and treatment, M. Nageeb Rashed, IntechOpen
- Tuncer, M., & Ozdemir, B. (2014). Photocatalytic activity of TiO₂ powders synthesized by supercritical gas antisolvent method. *ACTA PHYSICA POLONICA A*, 125(2), 608–610.
- Yao, C., Chen, W., Li, L., Jiang, K., Hu, Z., Lin, J., Xu, N., Sun, J., & Wu, J. (2021). ZnO: Au nanocomposites with high photocatalytic activity prepared by liquid-phase pulsed laser ablation. *Optics & Laser Technology*, 133, 106533. <https://doi.org/10.1016/j.optlastec.2020.106533>
- Yassitepe, E., Yatmaz, H. C., Öztürk, C., Öztürk, K., & Duran, C. (2008). Photocatalytic efficiency of ZnO plates in degradation of azo dye solutions. *Journal of Photochemistry and Photobiology a: Chemistry*, 198(1), 1–6.
- Zhang, X., Yuan, J., Zhu, J., Fan, L., Chen, H., He, H., & Wang, Q. (2019). Visible light photocatalytic performance of laser-modified TiO₂/SnO₂ powders decorated with SiC nanocrystals. *Ceramics International*, 45, 12449–12454. <https://doi.org/10.1016/j.ceramint.2019.03.178>
- Zhu, D., Wang, L., Yu, W., & Xie, H. (2018). Intriguingly high thermal conductivity increment for CuO nanowires contained nanofluids with low viscosity. *Scientific Reports*, 8, 5282. <https://doi.org/10.1038/s41598-018-23174-z>

Publisher's Note Springer Nature remains neutral with regard to jurisdictional claims in published maps and institutional affiliations.